

1 **Modeling of radon exhalation from soil influenced by environmental**  
2 **parameters**

3

4 Jinmin Yang<sup>1,2#</sup>, Hannah Busen<sup>3</sup>, Hagen Scherb<sup>3</sup>, Kerstin Hürkamp<sup>1</sup>, Qiuju Guo<sup>2</sup>, Jochen  
5 Tschiersch<sup>1\*</sup>

6

7 <sup>1</sup> Helmholtz Zentrum München, Institute of Radiation Protection, 85764 Neuherberg,  
8 Germany

9 <sup>2</sup> State Key Laboratory of Nuclear Physics and Technology, Peking University, 100871  
10 Beijing, China

11 <sup>3</sup> Helmholtz Zentrum München, Institute of Computational Biology, 85764 Neuherberg,  
12 Germany

13

14

15 \* Corresponding author.

16 Helmholtz Zentrum München (GmbH)  
17 German Research Center for Environmental Health  
18 Institute of Radiation Protection  
19 Ingolstädter Landstr. 1  
20 85764 Neuherberg, Germany

21 E-Mail: [tschiersch@helmholtz-muenchen.de](mailto:tschiersch@helmholtz-muenchen.de)

22 Phone: +49 89 31872763

23 Fax: +49 89 31873363

24

25 # Present address:

26 Sino-French Institute of Nuclear Engineering and Technology, Sun Yat-sen University,  
27 519082 Zhuhai, Guangdong, China

28

29 JY: [jinmin.yang@pku.edu.cn](mailto:jinmin.yang@pku.edu.cn)

30 HB: [hannah.busen@helmholtz-muenchen.de](mailto:hannah.busen@helmholtz-muenchen.de)

31 KH: [kerstin.huerkamp@helmholtz-muenchen.de](mailto:kerstin.huerkamp@helmholtz-muenchen.de)

32 QG: [qjguo@pku.edu.cn](mailto:qjguo@pku.edu.cn)

33 JT: [tschiersch@helmholtz-muenchen.de](mailto:tschiersch@helmholtz-muenchen.de)

34



58 1. INTRODUCTION

59

60 Radon (Rn-222) is one of the most important naturally occurring radioactive elements  
61 and contributes to more than half of the ionizing radiation exposure of humans (UNSCEAR,  
62 2000). Its adverse health effect is well approved (WHO, 2009). Radon originates from miner-  
63 al grains, which contain the parent nuclide radium (Ra-226) by recoil and diffusion mecha-  
64 nisms. A part of radon, which is produced mainly on the surface layer of the minerals can  
65 eject out of the grains and may emanate into the interstitial space between them. These radon  
66 atoms exist in gaseous form and spread into the pore space driven by diffusion and advection.  
67 They are dominantly transported by carrier fluids, whereas the radon migration depends upon  
68 the fluid flow characteristics of the soil. Some radon gas will eventually migrate upwards to  
69 the soil/air interface and exhales out into the atmosphere. The exhalation rate of soil radon  
70 gives the source strength of radon into the atmosphere. The characterization of this transfer  
71 process is crucial for the understanding of the following fate of the radioactive rare gas: either  
72 as trace substance in atmospheric dispersion or as accumulating contaminant in the indoor  
73 environment. This importance made it to an intense subject of investigations.

74

75 Former studies have revealed that the radon exhalation process is influenced by vari-  
76 ous environmental parameters. An overview is given e.g. by Nazaroff (1992) or recently by  
77 Sakoda and Ishimori (2017). Many investigators have observed that low soil water content  
78 promotes exhalation while abundant wetness depresses the exhalation (Schery et al., 1989;  
79 Strandén et al., 1984; Zhuo et al., 2006). Seasonal variations exist with higher exhalation rates  
80 in dry summers and autumns and lower ones in rainy winters and springs (King and Minis-  
81 sale, 1994). Strandén et al. (1984) have reported a weak positive effect of soil temperature on  
82 the exhalation rate and Iskandar et al. (2004) presented a formula indicating a positive linear  
83 correlation between radon emanation power and soil temperature. This is plausible since the  
84 increase of soil temperature can reduce the portion of radon adsorbed on soil grains. Therefore,  
85 the emanation is enhanced. Moreover, an increasing temperature can promote the radon diffu-  
86 sion process. However, most of the former studies have investigated only either the soil tem-  
87 perature or the air temperature. Note that under stable laboratory experimental conditions, the  
88 air and the soil temperature are nearly the same. It is unclear whether the influencing-  
89 mechanism of air and soil temperature are similar and in the same direction. But in the natural  
90 environment, the air temperature fluctuates more fiercely and may thus be rather different  
91 from the soil temperature. Therefore, models implementing both, air and soil temperature,  
92 would be necessary to fill the gap. In addition, the exhalation might be expected to increase

93 when the air pressure decreases. The pressure difference is an important driving force of the  
94 gas transport in the indoor environment, where significant differences between in- and out-  
95 door air pressure occur..

96

97 Besides, soil properties such as the grain size as well as the radium content and its dis-  
98 tribution in the grains, which is responsible for different emanation patterns (Chau et al.,  
99 2005; Chitra et al., 2018; De Martino et al., 1998), precipitation (Ferry et al., 2001; Müllerova  
100 et al., 2018) and air pressure (Koarashi et al., 2000) also play an important role in the exhala-  
101 tion process. It is well known that water in the soil space affects both, radon emanation and  
102 diffusion (Hassan et al., 2009; Sakoda et al., 2011). On one side, when the radon atoms eject  
103 out of the soil grain, water can help retain them in the pore space. On the other side, the radon  
104 diffusion coefficient for water is fairly smaller than that for air (Tanner, 1980) and the redun-  
105 dant soil water content would block the diffusion path and suppresses the exhalation. Overall,  
106 the promotion effect is dominant when the soil is relative dry; when the soil gets moist, the  
107 depression effect becomes prominent.

108

109 Most of the former studies were based on laboratory techniques and focused on single-  
110 variable effects. However, the laboratory experimental conditions, e.g. by means of disturbed  
111 sample material or controlled ambient conditions, could be far different from the field ambi-  
112 ance and would give rise to quite different results (Papachristodoulou et al., 2007). Moreover,  
113 the numerous influencing factors affect the exhalation not only directly, but also indirectly by  
114 modulating other relevant factors. Therefore, field measurements are needed to investigate  
115 how pertinent the impact of environmental parameters on the exhalation process is. Another  
116 advantage of *in situ* measurements is the possibility of performing long-term monitoring stud-  
117 ies of the exhalation rate and the influence of seasonal variations on meteorological condi-  
118 tions and soil properties. In our study, a self-developed automatic measurement system called  
119 exhalometer (Yang et al., 2017), which is similar to a system used by Mazur and Kozak  
120 (2014), was applied for the continuous measurement of the Rn-222 exhalation rate from soils  
121 for two years, 2015 and 2016.

122

123 The aim of the investigation was to test the impact of the environmental parameters on  
124 the radon exhalation process. For the first time a two years time record of the exhalation rate  
125 is available for statistical analysis. In addition, environmental parameters as soil characteris-  
126 tics, soil water content and meteorological parameters were recorded over the same period. In  
127 a first step, the response of the exhalation rate to soil water content was modeled by a parsi-

128 monious 2-parameter Rayleigh function and the corresponding shape and scale parameters  
129 were estimated. In a second step, together with the remaining environmental parameters, the  
130 Rayleigh transformed soil humidity is then included in a linear multivariate autoregressive  
131 model of the radon exhalation. By this, the importance of single parameters to explain the  
132 radon exhalation variability as well as the forecasting performance of the multivariate model  
133 was elaborated.

134

## 135 2. MATERIALS AND METHODS

### 136 **2.1 Study site, soil characterization and measurement of environmental parameters**

137 Measurements were carried out on an open grassy field at the campus of Helmholtz  
138 Zentrum München, about 10 km north of the city of Munich (493 m a.s.l., 48°13'N, 11°36'E).  
139 The location can be described as a typical semi-rural area in southern Bavaria. The prevalent  
140 wind is from western direction and the amount of mean annual precipitation is 834 mm  
141 (1981-2010). The site is located on the Munich gravel plain, an up to 100 m thick Pleistocene  
142 glacial outwash plain that developed during the last three ice ages and covers 1500 km<sup>2</sup> of the  
143 Bavarian alpine forelands. Mainly calcareous gravels (<1-2% crystalline rocks) were trans-  
144 ported by glaciers from the central and northern Alps and accumulated due to subsequent melt  
145 water transport on fluvial terraces in the alpine forelands. On site, in 8-10 m well-rounded  
146 gravels, shallow pararendzinas developed, mainly consisting of 10 cm humic topsoils and  
147 transitional horizons to the underlying unconsolidated bedrock material of maximum the same  
148 thickness. At the same site radon soil gas measurements were performed previously (Bunzl et  
149 al., 1998).

150

151 For a sedimentological characterization of the site and the analysis of the specific ac-  
152 tivity of Ra-226 in the sediments, four soil samples of 15-20 cm depth were collected arbitrar-  
153 ily around the measurement field (Table 1, sample no. 1-4). In addition, two depth-integrated  
154 samples were taken from a shallow soil profile separately for the humic topsoil (0-10 cm, no.  
155 5) and the weathered bedrock horizon below (10-22 cm, no. 6). The sampling depths of the  
156 five subsoil samples correspond to the depths of the soil water content measurements. Bulk  
157 soil densities were determined by taking the weight of three volume-related samples, grain  
158 densities by applying the pycnometer method on the same samples (Flint and Flint, 2002).  
159 Porosities were calculated from the ratio of both densities. After drying the samples at 105°C  
160 in an oven, the fraction <2 mm was separated by sieving for the determination of the CaCO<sub>3</sub>  
161 content (DIN 18129, 2011) and specific activity of Ra-226 by gamma-spectrometry for all

162 samples. Analyses for the grain size distribution according to ISO 11277 (2009) were per-  
163 formed on another two samples from 0-10 cm and 10-22 cm depth in the soil profile, referred  
164 to as no. 7 and 8 in Table 1.

165  
166 The samples were transferred to plastic cups and left for three weeks before gamma  
167 spectrometric measurement to achieve a secular equilibrium of Ra-226 and its progeny. The  
168 Ra-226 activity was determined by integrating the areas of the full energy peaks at 186.2 keV  
169 and at the energies of the progeny Pb-214 (295.2 keV and 351.9 keV) and Bi-214 (609.3 keV  
170 and 1764.5 keV). Measurement times for the samples no. 1-6 were between 24 h and 15.5 d in  
171 order to diminish the analytical uncertainty to less than 8%. For the samples no. 7-8 uncer-  
172 tainties for the size fractions <2 mm were slightly higher, because the grain size analytical  
173 method provided only small amounts of sample material (2-5 g) for gamma-spectrometric  
174 measurements. Corrections for the self-attenuation according to Cutshall et al. (1983) and for  
175 the overlap of the energy peak of Ra-226 at 186.2 keV with that of U-235 at 185.7 keV were  
176 carried out.

177  
178 Parallel to the continuous measurement of the radon exhalation rate (see chapter 2.2),  
179 the environmental parameters air temperature, soil temperature in 20 cm depth, air pressure,  
180 the amount of precipitation, humidity, wind intensity and direction were recorded at the  
181 measurement site. Soil water content was determined in 10-20 cm depth with an ECH<sub>2</sub>O EC-5  
182 sensor (Decagon Devices). It logged the volumetric water content by the dielectric constant of  
183 the media using capacitance/frequency (70 MHz) domain technology (e.g., Kizito et al., 2008;  
184 Kodešová et al., 2011) every minute. Hourly means were calculated for further evaluation.  
185 The accuracy was improved to 1-2% uncertainty by carrying out a calibration of the sensor  
186 with soil material from the study site at defined soil water content in the laboratory.

187

## 188 **2.2 Exhalometer for the measurement of the radon exhalation rate**

189 An automatic measurement system called exhalometer was developed for the long-  
190 term radon exhalation rate measurement during the years 2015 and 2016. It is based on the  
191 accumulation method. A bottom opened cylinder hood with diameter 40 cm and height 35 cm  
192 is adopted as the accumulation chamber. During the sampling time of 1 h, the accumulation  
193 chamber seals onto a collar which is inserted into the soil. The gas sample in the hood is  
194 transported into six Lucas scintillation cells successively. With the build-up curve of the ra-  
195 don concentration in the accumulation chamber, the exhalation rate  $E$  (Bq m<sup>-2</sup> h<sup>-1</sup>) can be de-

196 terminated according equation (1) through the subsequent measurement of the increasing radon  
197 concentration with time:

$$198 \quad C(t) = C_0 + \frac{EA}{V}t \quad (1)$$

199 where  $C$  ( $\text{Bq m}^{-3}$ ) is the time-dependent radon concentration in the chamber,  $C_0$  ( $\text{Bq m}^{-3}$ ) is  
200 the initial radon concentration,  $A$  ( $\text{m}^2$ ) is the area of the chamber bottom,  $V$  ( $\text{m}^3$ ) is the volume  
201 of the chamber and  $t$  is the radon accumulation time (Yang et al., 2017). Due to the short half-  
202 life of thoron (56s), a low quasi-stable thoron concentration in the accumulation chamber will  
203 establish soon. As a contribution to  $C_0$  it will not influence the radon exhalation results.

204

205 After sampling, the hood is lifted up and moves off the sampling area for three hours  
206 in order to keep the soil surface consistent with ambiance. Details about the experiment setup,  
207 measurement cycles and the calculation of the exhalation rates are given in Yang et al. (2017).

208

### 209 **2.3 Data and statistical modeling**

210 The radon exhalation is affected by a variety of environmental parameters and the  
211 amount and distribution of the radon's parent nuclide Ra-226 in the soil. In our study, the soil  
212 water content, soil temperature, air humidity, air temperature, air pressure, precipitation, wind  
213 speed and wind directions were recorded. Preliminary correlation and regression analyses  
214 indicated that the air temperature, the soil temperature in 20 cm depth, the soil water content  
215 and the air pressure most dominantly affect the radon exhalation rate compared to the other  
216 measured variables. Therefore, the applied statistical model is based on these four parameters  
217 and can be expressed as

$$218 \quad E = \alpha_0 + \alpha_1 w + \alpha_2 T_s + \alpha_3 T_a + \alpha_4 P + \sum \beta_k E_k \quad (2)$$

219 with  $E$  = exhalation rate,  $w$  = volumetric soil water content,  $T_s$  = soil temperature in 20 cm  
220 depth,  $T_a$  = air temperature,  $P$  = air pressure,  $\alpha_i$  ( $i = 1, 2, 3, 4$ ) = regression coefficients,  $E_k$  ( $k$   
221 = 1, 2 ...) = exhalation rate of the  $k^{\text{th}}$  previous measurement cycle and  $\beta_k$  = regression coeffi-  
222 cients of lagged variables.

223

224 In the regression model, it is assumed that all variables have a linear relationship with  
225 the radon exhalation rate. Due to nonlinear dual influences of the soil water content, a linear  
226 fit is inappropriate in the regression model. In this case, the linear function is substituted by a  
227 Rayleigh type function. The Rayleigh function  $R(w)$  provides an elegant and parsimonious

228 parametrization and is determined (up to an intercept) by the parameters  $b$  and  $c$ : the inflec-  
229 tion point  $c$  is the location of the global maximum:

$$230 \quad R(w) = E(w) = \frac{bwe^{\frac{1}{2}(1-\frac{w^2}{c^2})}}{c} \quad (3)$$

231 where  $E(w)$  is the exhalation rate and  $w$  is the volumetric soil water content.

232

233 Except from the dependence on environmental parameters, the radon exhalation rate  
234 has a distinct autocorrelation. The measurement cycle of the radon exhalation rate in this  
235 study took four hours. Generally, all environmental parameters that might affect the exhala-  
236 tion process would not change too much within that period. Consequently, it is assumed that  
237 also the exhalation rate would not change drastically either. It is supposed, that the previous  
238 measurement can deliver some predictive value for the subsequent one. This implies that sev-  
239 eral previous data points can be used to estimate the next data point, which was applied for  
240 lag1, lag3, and lag5 (first, third and fifth measurement value before) in the autocorrelation  
241 analysis.

242

243 The data sets generated contain 1625 recorded values from January 2<sup>nd</sup> to December  
244 31<sup>st</sup>, 2015 and 941 measurements from February 19<sup>th</sup> to October 17<sup>th</sup>, 2016. It sums up to four  
245 to five exhalation rate readings per day in 2015 and approximately four readings per day in  
246 2016. For the data processing, statistical analyses, and results display, Microsoft Excel 2013,  
247 R 3.2.1, Origin 8 (OriginLab Corporation), Wolfram MATHEMATICA 10.4, and SAS/STAT  
248 software 9.4 (SAS Institute Inc., 2014) was used.

249

## 250 3. RESULTS AND DISCUSSION

### 251 3.1 Soil characterization

252 As the radon exhalation rate mainly depends on the amount and distribution of its par-  
253 ent nuclide Ra-226 in the sediments, soils at the measurement site are characterized by the  
254 analysis of typical sedimentological parameters, which confirms the fluvio-glacial origin of  
255 the accumulated sediments. The grain size analysis (Table 1) proves that the subsoil sedi-  
256 ments (10-22 cm depth) are dominated by 68% gravel and 26% sand; they are very poor in  
257 silt and clay (6%). The content of clay is only about 1.5%. The separate analysis of the total  
258 fraction of fine material (<2 mm) defines the sediment as a slightly loamy sand. However, the



259 under-representation of the fraction <2 mm results in a comparably high porosity and high  
260 water permeability. It also leads to short-term full water saturation of the soil immediately  
261 after strong precipitation events. Calcium carbonate contents are 33% in the topsoil and 37%  
262 in the layer 10-22 cm. Soil water contents in these two samples were 7.0% and 9.0%, respec-  
263 tively, on the day of sampling. The mean bulk and grain density was  $1.39 \text{ g cm}^{-3}$  and  $2.45 \text{ g}$   
264  $\text{cm}^{-3}$ , respectively. The densities are in the range of typical values for well-permeable sandy  
265 soils. The porosity is calculated with a high mean value of 0.43 and therefore is in the upper  
266 ranges for typical unconsolidated sediments.

267

268 The specific activities of Ra-226, being the parent nuclide of Rn-222, are shown in  
269 Table 1. The specific activities of the bulk soil samples <2 mm range between  $50\text{-}131 \text{ Bq kg}^{-1}$   
270 indicating the heterogeneity of the Ra-226 distribution over the measurement site. The analy-  
271 sis of grain-size-fractionated samples no. 7 and 8 proves an increase of Ra-226 contents with  
272 decreasing grain sizes and increasing specific surface areas of each grain. Higher radon ema-  
273 nation factors for sediments with grain sizes <0.2 mm were already discussed by Chitra et al.  
274 (2018). It is worth noting that the measurements of medium and coarse gravels have higher  
275 gamma-spectrometric measurement uncertainties than those given in Table 1. The listed val-  
276 ues for the specific activities depend on the mineralogical composition of single gravels that  
277 were selected for measurement due to limited space in the 250 mL calibrated measurement  
278 cups.

279

280 Differences in the specific Ra-226 activities between the samples of the two different  
281 depths in the soil profile are low. Since grain size distributions in both layers are already  
282 comparable, also a similar distribution of Ra-226 activities over depth can be expected.

283

284

### 285 **3.2 Modeling results**

286 The radon exhalation rate is relatively low for dry and wet soils and is relatively high for in-  
287 termediate soil water content. In a first step, therefore, we modeled this behavior by a pars-  
288 monious 2-parameter Rayleigh function and estimated the corresponding shape and scale pa-  
289 rameters  $b$  and  $c$ , respectively (see equation (3)). The non-linear Rayleigh-transformed soil  
290 humidity entails a much better overall model fit than just the direct (linear) soil humidity  
291 alone when comparing the Akaike Information Criterion (AIC). In a second step together with  
292 the remaining environmental parameters, the Rayleigh transformed soil humidity is then in-

293 cluded in a linear multivariate autoregressive model of the radon exhalation. The approach is  
294 based on a parsimonious so to speak ‘hybrid’ partially nonlinear autoregressive model. More  
295 sophisticated and less parsimonious models yielded not much better results. Moreover, in-  
296 cluding lagged co-variable measurement values did not improve the model significantly.

### 297 *3.2.1 Dependence of the radon exhalation rate on soil water content– univariate modeling*

298 The measured radon exhalation rates in dependence of the volumetric soil water con-  
299 tent are shown in Figures 1-3 for the years 2015, 2016, and for both years combined, respec-  
300 tively. The exhalation rates range up to  $80 \text{ Bq m}^{-2} \text{ h}^{-1}$  with a mean of  $25.3 \text{ Bq m}^{-2} \text{ h}^{-1}$  and  
301 therefore in the range of typical values that can be found in literature for short term measure-  
302 ments (NCRP, 1988, Porstendörfer, 1994, UNSCEAR, 2000). Using Equation (3) to describe  
303 the exhalation rate from the soil water content, the best estimates of the model parameters are  
304 shown in Table 2. The value of the soil water content inflection point  $c$  varies between 8.4%  
305 (2015) and 13% (2016) with an average value of 10% for both years 2015 and 2016 combined.  
306 Therefore, the soil water content inflection point is consistent with findings from other studies  
307 (Bossew, 2003; Hosoda et al., 2007; Schery et al., 1989; Zhuo et al., 2006). However, the R-  
308 square obtained by univariate modeling is rather low in the range of only 6-18%. The data are  
309 roughly divided into two stages. When the soil is relatively dry, the exhalation tends to in-  
310 crease along with the water saturation. After the inflection point at 8% in 2015 and 13% in  
311 2016, the exhalation rate decreased to approximately one third with an increase in the soil  
312 water content to 24% (Figure 3). Water works to promote radon exhalation up to a certain  
313 water content and retains the Rn-222 afterwards. The effect of water content on the radon  
314 exhalation may be dominated by two processes. (a) Diffusion occurs in air-filled pores at low  
315 water contents and radon is distributed between air and water at equilibrium. The partition  
316 between gas and liquid phase depends on the relative volume of water in the pore space caus-  
317 ing higher concentrations in the gas phase when the water content increases. In addition, ema-  
318 nating radon molecules from the soil grains have a greater probability to stay in the pore space  
319 if the density is higher with increasing water content. The radon concentration in the air-filled  
320 soil pore space is higher due to partitioning and increased emanation at higher water content..  
321 (b) Diffusion occurs dominantly in water-filled pores at high water contents and air/water  
322 equilibrium only exists near interfaces. Under these conditions, the radon concentration in soil  
323 air can be low (Faheem and Matiullah, 2008).

324

325

326 3.2.2 Multivariate modeling

327 It is interesting to consider whether the quality of the fit function of the univariate  
328 model can be improved by including further environmental parameters as well as significant  
329 variables accounting for the strong autocorrelation in the exhalation rates (Figure 4). There-  
330 fore, the soil temperature in 20 cm ( $T_s$ ), the air temperature ( $T_a$ ), the air pressure ( $P$ ), as well  
331 as lag1 (n-1), lag3 (n-3), and lag5 (n-5) (previous first, third and fifth) of the exhalation meas-  
332 urements were added to the regression model. Lag2 and lag4 both explained less variability  
333 and conveyed larger p-values than lag3 and lag5 in conjunction with the combined lag0 (=   
334 original exhalation) and lag1. Therefore only lag1, lag3 and lag5 were introduced. The result-  
335 ing parameters and confidence limits for both years combined are compiled in Table 3. The  
336 R-square increases to 61%. Figure 5 presents pertinent regression diagnostics, which shows  
337 an overall reasonable fit quality together with approximately normally distributed residuals. In  
338 general the normal quantile-quantile plot demonstrates if the residuals are normal distributed.  
339 If this is the case, all residuals follow the diagonal line. In our case this is not given exactly  
340 for the lower and higher quantiles, but the middle region fits very well. Also the histogram for  
341 the residual distribution shows that it fits quite well to the theoretical normal distribution.  
342 Therefore, the fitting function can be improved as:

$$E(n) = 3.00 + 0.18 * R(w) - 0.62 T_s + 0.52 T_a - 0.0002 P +$$

343  $0.49 E(n - 1) + 0.14 E(n - 3) + 0.18 E(n - 5)$  (4)

344 wherein  $R(w)$  is the Rayleigh transformed volumetric soil water content according to equation  
345 (3) and according the parameters in Table 2 for the combined years 2015 and 2016.

346

347 In Table 3, the insignificant level of the air pressure parameter indicates that the pres-  
348 sure is not important in the present data and the modeling context. This finding is supported  
349 by the investigation of Mazur and Kozak (2014) although their study was shorter (only one  
350 year). The reason for the insignificance of the air pressure might be the relatively slow change  
351 over a large area. Maybe the pressure difference between atmosphere and soil at a certain  
352 depth might be a better parameter. The closed accumulation chamber during sampling might  
353 reduce the influence of the external air pressure as well.

354

355 A rise of temperature has been thought to linearly increase the radon emanation (Is-  
356 kandar et al., 2004). This may be due to a reduction in physical adsorption of radon onto  
357 grains that occurs during the diffusion through the porous material (Sakoda et al., 2011;  
358 Strandén et al., 1984). The fitting results show distinct positive and negative effects of air and

359 soil temperature, respectively. This is unexpected and it may imply a different influencing-  
360 mechanism of air and soil temperature. The negative effect of soil temperature contradicts the  
361 experimental results of some other studies (Iskandar et al., 2004; Schary et al., 1989; Stranden  
362 et al., 1984). Nevertheless, the theoretical calculation model by Sakoda and Ishimori (2014)  
363 has obtained a similar negative effect. The reason for the negative effect of the soil tempera-  
364 ture on the exhalation rate might be that the influence of soil temperature in the natural envi-  
365 ronment has a time delay. It takes some time for the radon gas to migrate to the soil surface.  
366 This delay may mask the real effect of soil temperature. Further research and data analyses  
367 are needed to explain the unexpected, however highly significant negative effect of the soil  
368 temperature.

369  
370 The simulation results are compared to measured exhalation rates in Figure 6. It is ob-  
371 vious that after considering the autocorrelation lag1, lag3, and lag5, the forecasting perfor-  
372 mance of the model has been improved considerably. The R-square increased from 28% (Fig-  
373 ure 6, upper graph) to 61% (Figure 6, lower graph). The simulated data is consistent with the  
374 measurement data, but the conformity weakens at very high and low exhalation rates  $>50 \text{ Bq m}^{-2} \text{ h}^{-1}$   
375 and  $<10 \text{ Bq m}^{-2} \text{ h}^{-1}$ . The autocorrelation functions show distinct autocorrelation for all  
376 involved variables (Figure 7). For the independent variables the autocorrelation vanishes after  
377 a lag of approximate 100 measurements, which corresponds to approximately three weeks. In  
378 contrast, the independent exhalation variable vanishes only after 500 measurement cycles,  
379 which corresponds to approximately four months.

380  
381 The predictive power of the model was tested as well with our model analogous to the  
382 ‘hold-one-out’ method. In the combined data from January 2015 to October 2016, a chosen  
383 calendar month is excluded (i.e. one or two months are discarded). Next, the model parame-  
384 ters are estimated from each of the resulting 12 reduced data sets and the correlations of the  
385 observed and predicted radon exhalation values for the excluded month(s) are computed. The  
386 results are presented in Table 4. Compared to the overall correlation of 0.78 between the ob-  
387 served and predicted values based on all data, the ‘hold-one-calendar-month-out’ method  
388 yields somewhat higher correlations for February to April, and partly considerably lower cor-  
389 relations for the other months. The correlations are especially low for January, November, and  
390 December since for these three months data were available for the year 2015 only.

391

392

393

394 4. CONCLUSIONS

395 Based on the field measurement data of 2015 and 2016, a statistical multivariate re-  
396 gression model involving soil water content, soil and air temperature and air pressure was  
397 established to fit the radon exhalation from soils. This model can explain about 61% of the  
398 exhalation variation. As the radon exhalation showed a strong autocorrelation, its implemen-  
399 tation improved the model tremendously.

400

401 The fitting model corroborates the compound effects of soil water content. The radon  
402 exhalation rate increases until the soil water content exceeds about 10%. At higher soil wet-  
403 ness, the exhalation decreases gradually. The model also revealed opposite effects of air and  
404 soil temperature on the exhalation rate, which implies their possible different influencing-  
405 mechanisms. The negative effect of soil temperature is contrary to some former studies and  
406 suggests that a time delay effect might exist, which is not visible in laboratory studies where  
407 air and soil temperature are similar. Further experiments and time series analyses testing the  
408 influencing mechanisms are needed.

409

410 Figure 5 and Figure 6 show that lower or higher extreme values of the radon exhala-  
411 tion are less well represented by our model compared to the intermediate radon exhalation  
412 rate measurement data. This might be due to some nonlinear influences of the independent  
413 variables, which aspect may be a topic for further research. The correlations in the last column  
414 of Table 4 suggest that the model and its predictive power may possibly be significantly im-  
415 proved if data is available for more extended periods of time.

416

417 ACKNOWLEDGMENT

418 This work was supported by CSC, the China Scholarship Council by funding the stay  
419 of one of the authors (JY) at HMGU for the experimental work. We thank A. Seidl (Technical  
420 University Munich, TUM) for the measurements of  $\text{CaCO}_3$  contents in the soil samples.

421

422

423 REFERENCES

- 424 Bossew, P., 2003. The radon emanation power of building materials, soils and rocks. Applied  
425 Radiation and Isotopes, 59: 389-392.
- 426 Bunzl, K., Ruckerbauer, F., Winkler, R., 1998. Temporal and small-scale spacial variability  
427 of  $^{222}\text{Rn}$  gas in a soil with high gravel content. Sci. Total Environ. 220: 157-166.
- 428 Chau, N.D., Chruściel, E., Prokólski, Ł., 2005. Factors controlling measurements of radon  
429 mass exhalation rate. Journal of Environmental Radioactivity, 82: 363-369.
- 430 Chitra, N., B. Danalakshmi, D. Supriya, I. Vijayalakshmi, S. Bala Sundar, K. Sivasubramani-  
431 an, R. Baskaran, and M. T. Jose, 2018. Study of Radon and Thoron exhalation from soil  
432 samples of different grain sizes. Applied Radiation and Isotopes 133: 75–80.
- 433 Cutshall, N.H., Larsen, I.L., Olsen, C.R., 1983. Direct analysis of  $^{210}\text{Pb}$  in sediment samples:  
434 self-absorption corrections. Nuclear Instruments and Methods 206: 309-312.
- 435 De Martino, S., Sabbarese, C., Monetti, G., 1998. Radon emanation and exhalation rates from  
436 soils measured with an electrostatic collector. Applied Radiation and Isotopes 49: 407-  
437 413.
- 438 DIN 18129, 2011. Baugrund, Untersuchung von Bodenproben – Kalkgehaltsbestimmung.  
439 Deutsches Institut für Normung DIN 18129:2011-07.
- 440 Faheem, M., Matiullah, M., 2008. Radon exhalation and its dependence on moisture content  
441 from samples of soil and building materials. Radiation Measurements 43: 1458–1462.
- 442 Ferry, C., Beneito, A., Richon, P., Robe, M.C., 2001. An automatic device for measuring the  
443 effect of meteorological factors on radon-222 flux from soils in the long term. Radiation  
444 Protection Dosimetry, 93: 271-274.
- 445 Flint, A.L., Flint, L.E., 2002. Particle Density, in Methods of Soil Analysis: Part 4 Physical  
446 Methods. Soil Science Society of America Book Series: Madison, Wisconsin, USA. p.  
447 230-233.
- 448 Hassan, N.M., Hosoda, M., Ishikawa, T., Sorimachi, A., Sahoo, S. K., Tokonami, S., Fukushi,  
449 M., 2009. Radon Migration Progress and Its Influence Factor; Review. Japanese Journal  
450 of Health Physics, 44: 218-231.

- 451 Hosoda, M., Shimo, M., Sugino, M., Furukawa, M., Fukushi, M., 2007. Effect of Soil Moisture  
452 Content on Radon and Thoron Exhalation. *Journal of Nuclear Science and Technology* 44: 664–672.  
453
- 454 Iskandar, D., Yamazawa, H., Iida, T., 2004. Quantification of the dependency of radon emanation  
455 power on soil temperature. *Applied Radiation and Isotopes*, 60: 971-973.
- 456 ISO 11277, 2009. Soil quality - Determination of particle size distribution in mineral soil material -  
457 Method by sieving and sedimentation. International Organization for Standardization ISO 11277:2009.  
458
- 459 King, C.-Y., Minissale, A., 1994. Seasonal variability of soil-gas- radon concentration in central  
460 California. *Radiation Measurements* 23: 683-692.
- 461 Kizito, F., Campbell, C. S., Campbell, G. S., Cobos, D. R., Teare, B. L., Carter, B., Hopmans,  
462 J.W., 2008. Frequency, electrical conductivity and temperature analysis of a low-cost  
463 capacitance soil moisture sensor. *Journal of Hydrology* 352: 367– 378.
- 464 Koarashi, J., Amano, H., Andoh, M., Iida, T., 2000. Estimation of Rn-222 flux from ground  
465 surface based on the variation analysis of Rn-222 concentration in a closed chamber.  
466 *Radiation Protection Dosimetry*, 87: 121-131.
- 467 Kodesova, R., Kodes, V., Mraz, A., 2011. Comparison of Two Sensors ECH<sub>2</sub>O EC-5 and  
468 SM200 for Measuring Soil Water Content. *Soil and Water Research* 6: 102–110.
- 469 Mazur, J., Kozak, K., 2014. Complementary system for long term measurements of radon  
470 exhalation rate from soil. *Review of Scientific Instruments* 85: 022104
- 471 Müllerova, M., Holy, K., Blahusiak, P., Bulko, M., 2018. Study of radon exhalation from the  
472 soil. *Journal of Radioanalytical and Nuclear Chemistry* 315: 237–241.
- 473 Nazaroff, W.W., 1992. Radon transport from soil to air. *Review of Geophysics* 30: 137-160.
- 474 NCRP, 1988. Measurement of Radon and Radon Daughters in Air. National Council on Radiation  
475 Protection and Measurements. Report No. 097.
- 476 Papachristodoulou, C., Ioannides, K., Spathis, S., 2007. The effect of moisture content on  
477 radon diffusion through soil: Assessment in laboratory and field experiments. *Health*  
478 *Physics*, 92: 257-264.

479 Porstendorfer, J., 1994. Properties and behaviour of radon and thoron and their decay prod-  
480 ucts in the air. *Journal of Aerosol Science*, 25: 219-263.

481 Sakoda, A., Ishimori, Y., 2014. Calculation of temperature dependence of radon emanation  
482 due to alpha recoil. *Journal of Radioanalytical and Nuclear Chemistry*, 299: 2013-2017.

483 Sakoda, A., Ishimori, Y., 2017. Mechanisms and Modeling approaches of radon emanation  
484 for natural materials. *Japanese Journal of Health Physics*, 52: 296-306.

485 Sakoda, A., Ishimori, Y., Yamaoka, K., 2011. A comprehensive review of radon emanation  
486 measurements for mineral, rock, soil, mill tailing and fly ash. *Applied Radiation and*  
487 *Isotopes*, 69: 1422-1435.

488 SAS Institute Inc., 2014. *SAS/STAT User's Guide*, Version 9.4, Cary NC.

489 Schery, S.D., Whittlestone, S., Hart, K. P., Hill, S. E., 1989. The Flux of Radon and Thoron  
490 from Australian Soils. *Journal of Geophysical Research-Atmospheres*, 94 (D6): 8567-  
491 8576.

492 Stranden, E., Kolstad, A.K., Lind, B., 1984. The influence of moisture and temperature on  
493 radon exhalation. *Radiation Protection Dosimetry*, 7: 55-58.

494 Tanner, A.B., 1980. Radon migration in the ground: a supplementary review. *National radia-*  
495 *tion environment*, 3: 5-56.

496 UNSCEAR, 2000. Sources and Effects of Ionizing Radiation. Report to the General Assem-  
497 bly, Volume I: Sources, United Nations Scientific Committee on the Effects of Atomic  
498 Radiation, New York.

499 WHO, 2009. WHO handbook on indoor radon: a public health perspective. World Health  
500 Organization (WHO, Eds. H. Zeeb, F. Shannoun), pp. 1-94.

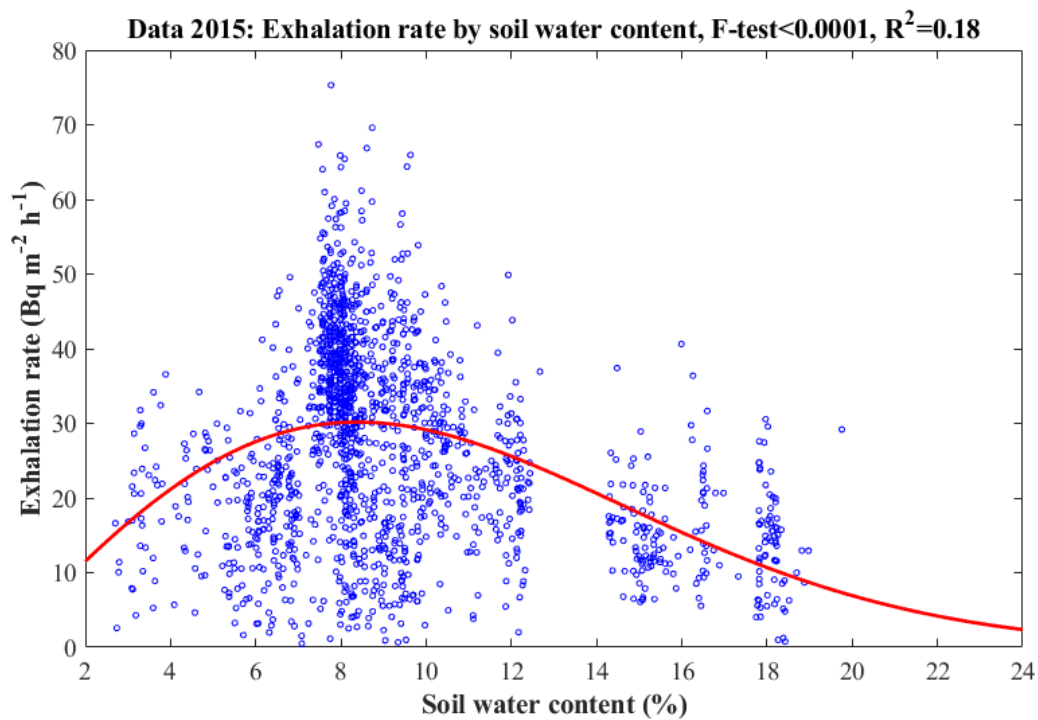
501 Yang, J., Buchsteiner, M., Salvamoser, J., Irlinger, J., Guo, Q., Tschiersch, J., 2017. Radon  
502 exhalation from soil and its dependence from environmental parameters. *Radiation Pro-*  
503 *tection Dosimetry* 177: 21-25.

504 Zhuo, W.H., Iida, T., Furukawa, M., 2006. Modeling radon flux density from the earth's sur-  
505 face. *Journal of Nuclear Science and Technology*, 43: 479-482.

506



508



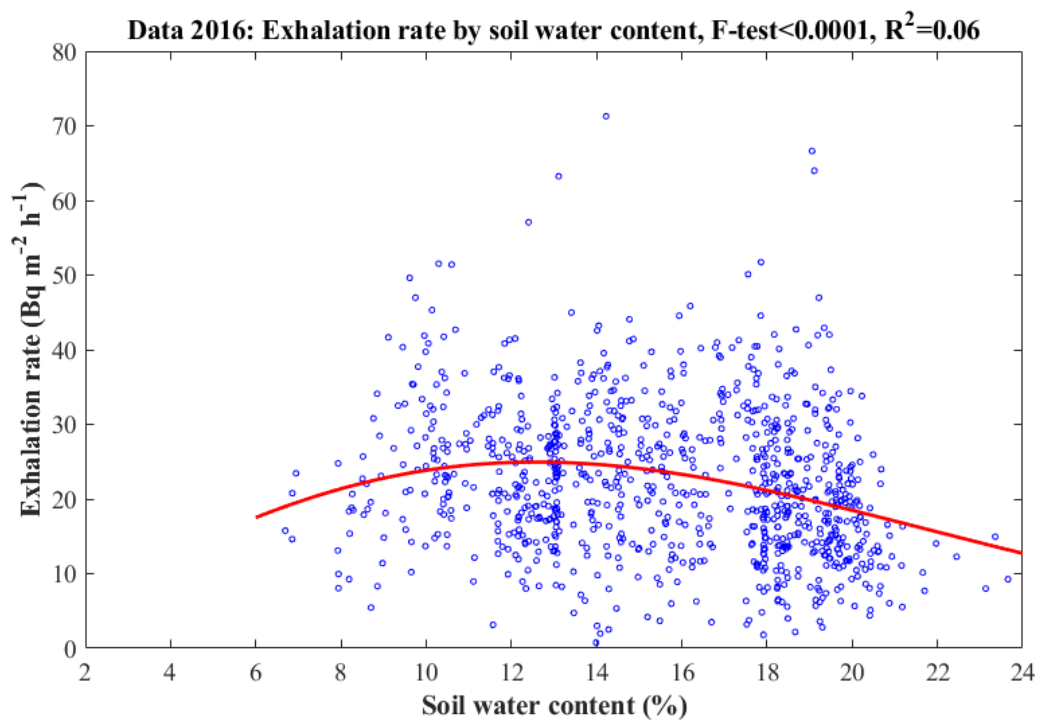
509

510

511

512 **Figure 1.** Variation of the radon exhalation rate with soil water content, data of 2015.

513



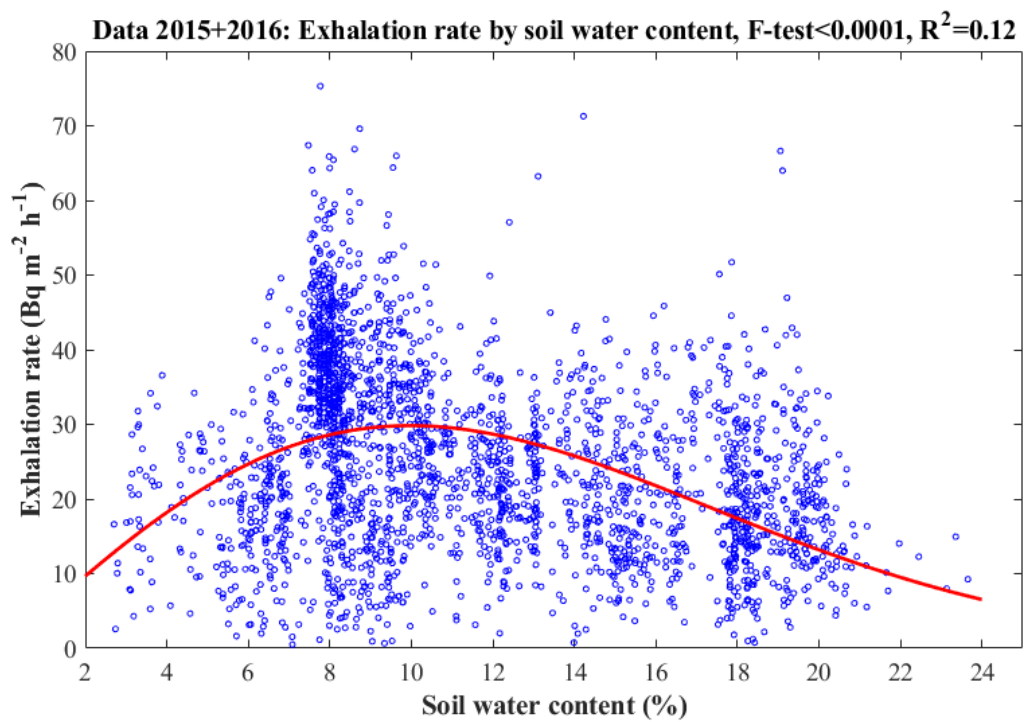
514

515

516

517 **Figure 2.** Variation of the radon exhalation rate with soil water content, data of 2016.

518



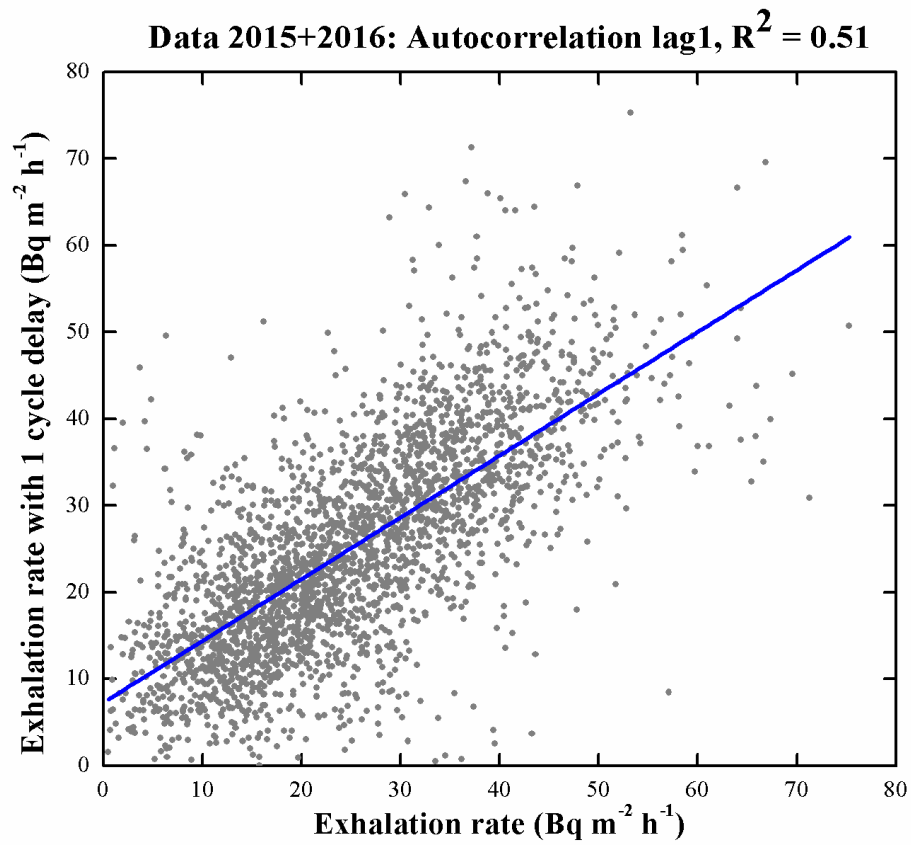
519

520

521

522 **Figure 3.** Variation of the radon exhalation rate with soil water content, data of 2015 and  
523 2016.

524



525

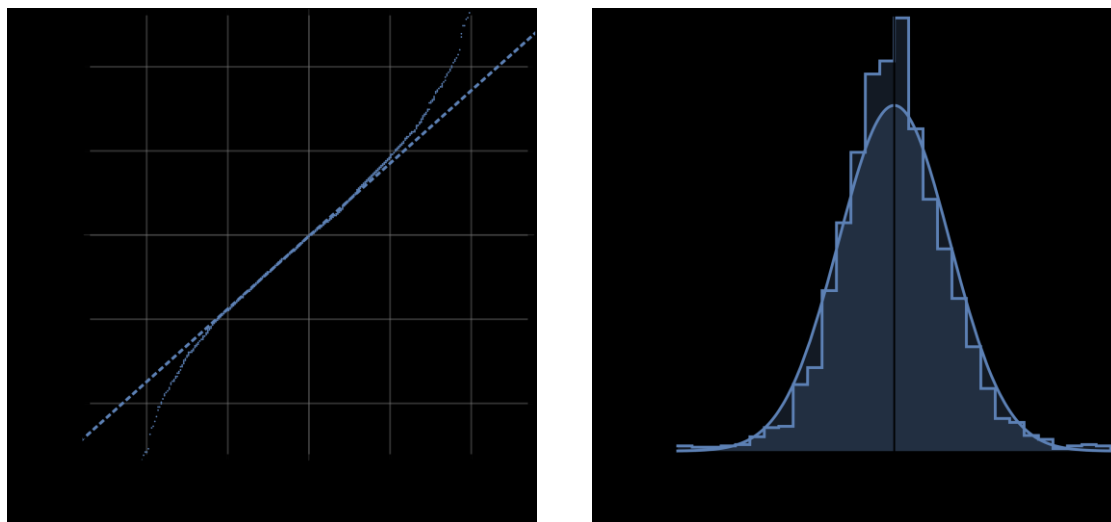
526

527 **Figure 4.** Autocorrelation scatter plot of the exhalation rate measurements versus the exhalation rate with lag1 (data of 2015 and 2016).

528

529

530



531

532

533 **Figure 5.** Fit diagnostics for the multivariate time-lagged environmental exhalation model  
534 with parameters listed in Table 3; left: quantile-quantile plot of the residuals; right: histogram  
535 distribution of the residuals compared to the fitted theoretical normal distribution.

536

537

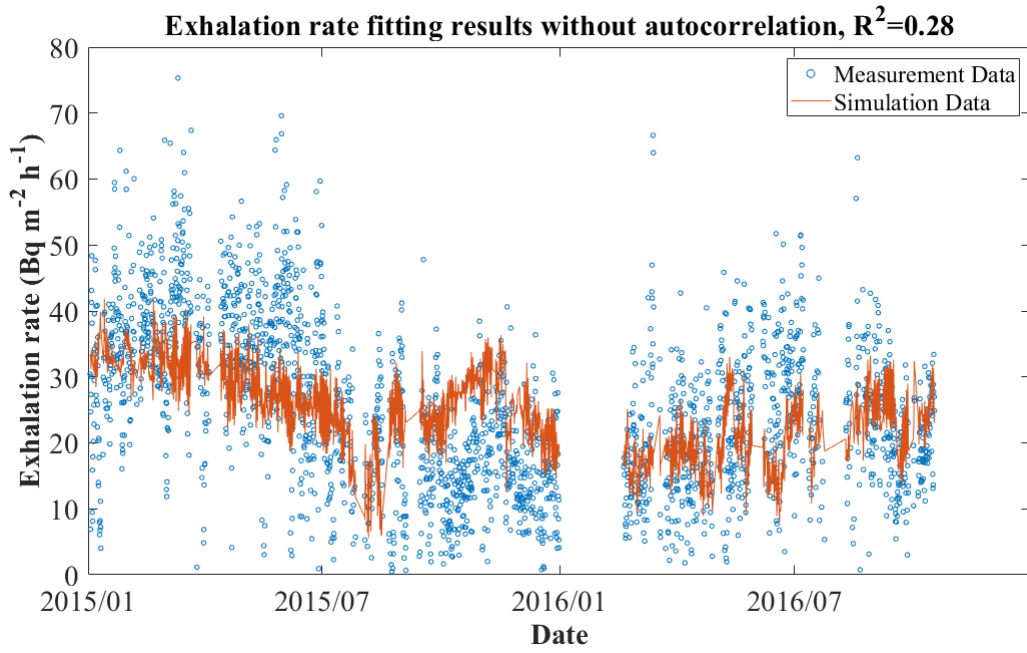
538

539

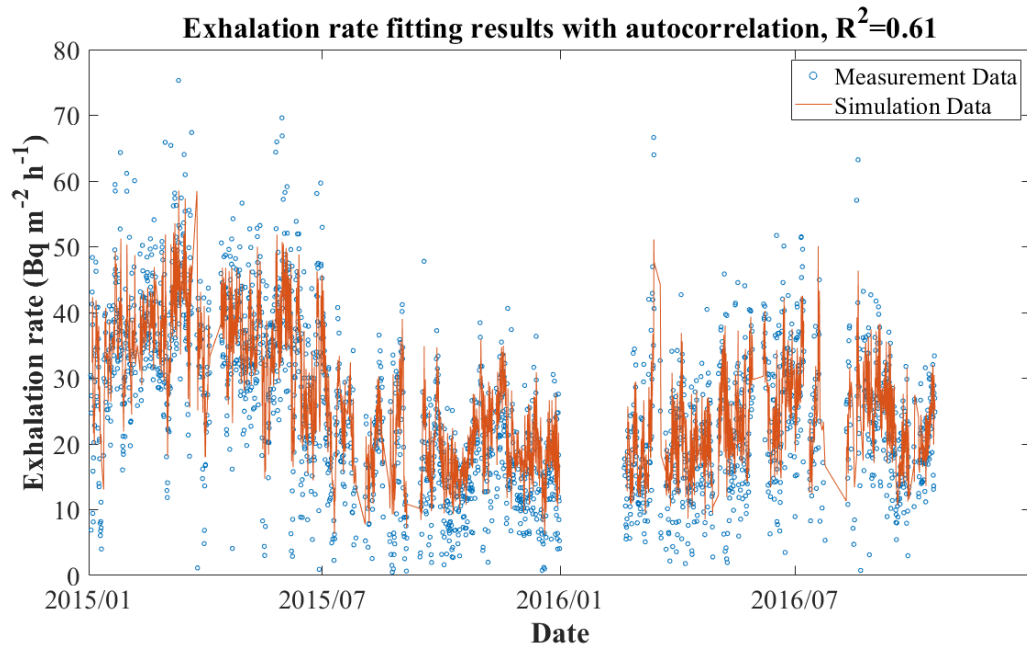
540

541

542



543

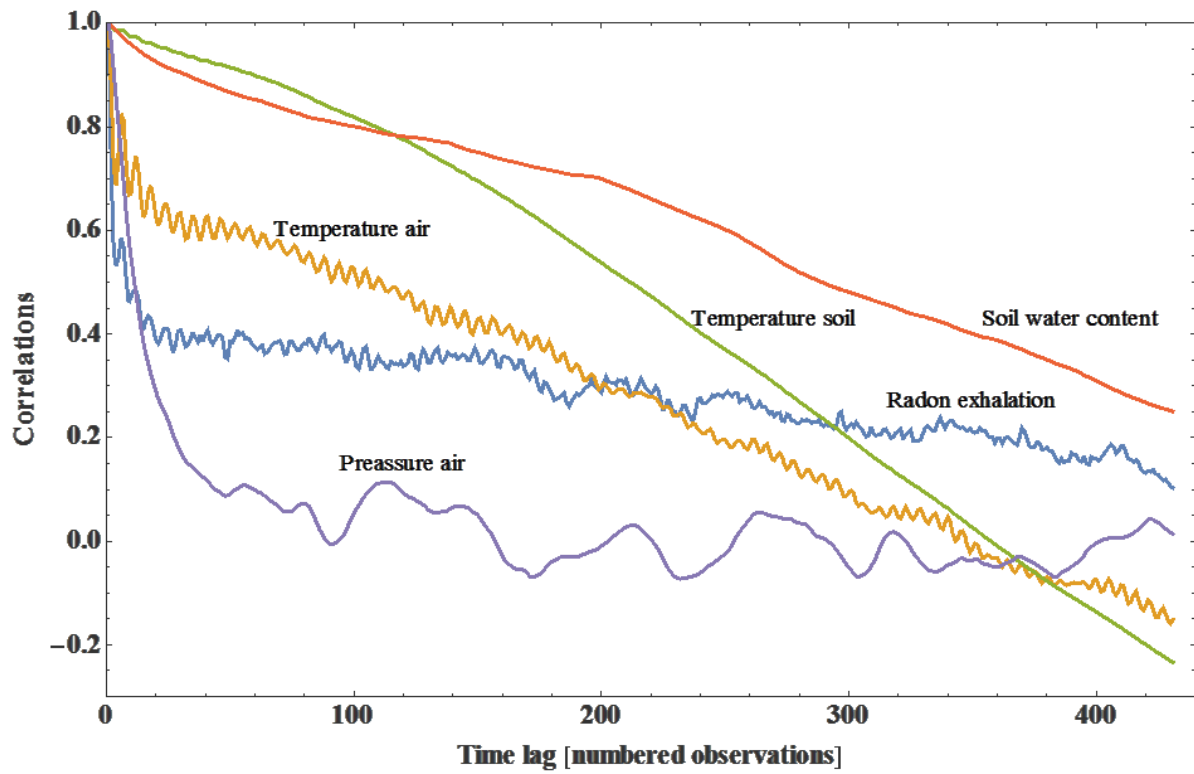


544

545

546

547 **Figure 6.** Simulation result of the multivariate time-lagged environmental exhalation model  
 548 in comparison to the experimental data. In the upper graph the simulation is shown without  
 549 considering the autocorrelation lag1, lag3 and lag5. In the lower graph the autocorrelation was  
 550 integrated in the model: the simulated data agree quite well with the measured data (except for  
 551 the extreme values) and R-square increased to 61%.



552

553

554 **Figure 7.** Autocorrelation functions for the radon exhalation and the environmental parameters studied.  
 555

556

557 **Table 1.** Grain size analysis and measured specific Ra-226 activities in the bulk fine material  
 558 < 2 mm (no. 1-6) and the size-fractionated soil samples (no. 7 and 8).

559

<b>Soil Sample No. (Depth)</b>	<b>Grain Size (mm)</b>	<b>Total Soil Mass (%)</b>	<b>Ra-226 Specific Activity (Bq/kg)</b>	<b>Ra-226 Uncertainty (Bq/kg)</b>
1 (15-20 cm)	<2		91.7	3.0
2 (15-20 cm)	<2		130.8	10.3
3 (15-20 cm)	<2		59.2	2.1
4 (15-20 cm)	<2		92.2	4.3
5 ( 0-10 cm)	<2		49.7	1.9
6 (10-22 cm)	<2		51.9	1.7
7 ( 0-10 cm)	coarse gravel	42.1	15.7	0.7
8 (10-22 cm)	(20-63)	22.6	16.2	0.7
7 ( 0-10 cm)	medium gravel	25.7	23.1	1.0
8 (10-22 cm)	(6.3-20)	27.7	23.8	1.1
7 ( 0-10 cm)	fine gravel	13.1	30.1	1.3
8 (10-22 cm)	(2-6.3)	17.8	35.6	1.6
7 ( 0-10 cm)	coarse sand	2.9	24.5	2.4
8 (10-22 cm)	(0.63-2)	5.1	27.3	4.1
7 ( 0-10 cm)	medium sand	7.1	21.4	2.6
8 (10-22 cm)	(0.2-0.63)	12.7	25.4	2.0
7 ( 0-10 cm)	fine sand	4.2	31.3	4.4
8 (10-22 cm)	(0.063-0.2)	8.2	37.2	6.0
7 ( 0-10 cm)	silt and clay	5.0	40.2	6.4
8 (10-22 cm)	(<0.063)	5.8	67.7	10.3

560

561



562 **Table 2.** Univariate modeling of radon exhalation by soil water content using Equation (3)  
563 with the parameters b and c for the years 2015, 2016 and the combined years 2015 and 2016.

564

<b>Year</b>	<b>Parameter</b>	<b>Estimate</b>	<b>Uncertainty</b>	<b>95% confidence limits</b>	
2015	b	30.2	0.3	29.5	30.8
	c	0.0839	0.0015	0.0810	0.0868
2016	b	24.9	0.4	24.1	25.8
	c	0.126	0.003	0.120	0.131
2015+2016	b	29.8	0.3	29.3	30.4
	c	0.0997	0.0010	0.0977	0.1018

565

566

567

568

569 **Table 3.** Multivariate modelling of radon exhalation with the best estimates of the model pa-  
570 rameters.

571

<b>Parameter</b>	<b>Estimate</b>	<b>Uncertainty</b>	<b>95% confidence limits</b>	
Intercept	3.01	19.56	-35.33	41.34
Soil water content	0.179	0.032	0.117	0.242
Temperature soil (20 cm)	-0.617	0.045	-0.705	-0.529
Temperature air	0.520	0.035	0.451	0.589
Pressure air	-0.002	0.020	-0.041	0.038
Lag1	0.492	0.016	0.460	0.523
Lag3	0.138	0.017	0.106	0.170
Lag5	0.177	0.016	0.144	0.209

572

573

574 **Table 4.** Assessment of the forecasting performance analogous to the ‘hold-one-out’ method. Parameter estimates of the combined non-linear and auto-  
 575 regressive linear regressions based on all data excluding any one chosen of all possible 12 calendar months and correlations between the observed and  
 576 predicted radon exhalation values in the month(s) excluded.

577

Month(s) in 2015 and 2016 excluded for model parameter estimation	Rayleigh parameters		Parameter estimates of the autoregressive linear regression								Correlation between the observed and predicted radon exhalation values in the month(s) excluded
	b	c	Intercept	Soil water content	Temperature soil	Temperature air	Pressure air	Lag1	Lag3	Lag5	
<b>None/Reference</b>	<b>29.833</b>	<b>9.975</b>	<b>3.005</b>	<b>0.179</b>	<b>-0.617</b>	<b>0.520</b>	<b>-0.002</b>	<b>0.492</b>	<b>0.138</b>	<b>0.177</b>	<b>0.78</b>
<b>January</b>	29.520	10.051	-14.226	0.185	-0.641	0.547	0.016	0.473	0.144	0.187	0.68
<b>February</b>	29.061	10.111	1.302	0.172	-0.611	0.539	0.000	0.487	0.138	0.179	0.82
<b>March</b>	28.846	10.016	35.671	0.182	-0.598	0.511	-0.035	0.494	0.138	0.171	0.80
<b>April</b>	29.275	9.996	3.938	0.177	-0.585	0.496	-0.003	0.494	0.140	0.181	0.81
<b>May</b>	29.267	9.960	12.374	0.182	-0.627	0.525	-0.011	0.495	0.122	0.188	0.66
<b>June</b>	29.356	9.818	4.348	0.179	-0.627	0.502	-0.003	0.485	0.147	0.178	0.64
<b>July</b>	30.057	9.895	4.570	0.180	-0.614	0.524	-0.003	0.491	0.140	0.174	0.71
<b>August</b>	30.080	9.939	1.284	0.180	-0.628	0.532	0.000	0.497	0.146	0.165	0.56
<b>September</b>	30.843	9.847	9.621	0.175	-0.574	0.491	-0.009	0.499	0.131	0.176	0.73
<b>October</b>	31.461	9.776	4.153	0.186	-0.608	0.504	-0.003	0.488	0.127	0.173	0.70
<b>November</b>	30.295	10.089	-6.336	0.211	-0.660	0.550	0.008	0.497	0.133	0.165	0.45
<b>December</b>	30.030	10.233	-30.933	0.167	-0.650	0.530	0.034	0.495	0.134	0.168	0.52

578

579